Turkish Journal of Science & Technology
18(1), 169-176, 2023

Research Paper
https://doi.org/10.55525/tjst.1219727

3-D Printed Dual-Band Frequency Selective Surfaces for Radome Applications

Mete BAKIR[1,2*]
[1] Makine Mühendisliği, Mühendislik ve Doğa Bilimleri Fakültesi, Ankara Yıldırım Beyazıt Üniversitesi, Ankara, Türkiye
[2] Malzeme Mühendisliği, Türk Havacılık ve Uzay Sanayii, Ankara, Türkiye
[*1] mete.bakir@aybu.edu.tr, [2] mete.bakir@tai.com.tr

(Geliş/Received: 15/12/2022; Kabul/Accepted: 21/02/2023)

Abstract: In this study, dual-band frequency selective surface (FSS) structures are designed by using 3-D printing technology for antenna radome applications. Four different configurations are studied to find the best alternative for FSS substrate not only for electromagnetic (EM) responses but also for its mechanical properties suitable for radomes. To ease the manufacturing process, a conductive paint is also studied instead of copper microstrip lines. In addition, graphite is also used for the comparison. Different 3-D printed configurations, various thickness values and three different materials for conductive part are examined and compared to find the most efficient radome structure.

Key words: 3-D Printer, Additive Manufacturing, Radome, Conductive paint, FSS.

Radom Uygulamaları için 3-B Baskılı Çift Bantlı Frekans Seçici Yüzeyler

Öz: Bu çalışmada anten radom uygulamaları için 3 boyutlu baskı teknolojisi kullanılarak çift bantlı frekans seçici yüzey (FSY) yapıları tasarlanmıştır. Sadece elektromanyetik (EM) tepkiler için değil, aynı zamanda radomlara uygun mekanik özellikleri için de FSY substratı için en iyi adayı bulmak üzere dört farklı konfigürasyon üzerinde çalışılmıştır. Üretim sürecini kolaylaştırmak için bakır mikroşerit hatların yerine iletken bir boya üzerinde de çalışılmıştır. Ayrıca karşılaştırma için grafit de kullanılır. En verimli radom yapısını bulmak için farklı 3-D baskılı konfigürasyonlar, çeşitli kalınlık değerleri ve iletken kısım için üç farklı malzeme karsilastirilmistir.

Anahtar kelimeler: 3-B yazicilar, eklemeli imalat, radom, iletken boya, FSY.

1. Introduction

With the developing technology, the production and manufacturing of materials have been improved with the help of 3-D printing technology in the material science area. As in Fused Filament Fabrication (FFF), Fused Deposition Modeling (FDM), Selective Laser Sintering (SLS), and PolyJetting, 3-D printing technology is based on layered production and additive manufacturing. The main advantage of 3-D printers is that very complex structures that cannot be manufactured in CNC machines can be designed and produced easily and in a very short time. 3-D printer technology has been started to be used in several areas from agriculture to the aerospace industry. 3-D printed materials also attract the scientific world and engineering industry in the electromagnetic field.

In this study, the application of 3-D printed materials in designing FSS structures was investigated. Frequency-selective surfaces (FSS) are composed of periodic resonators providing filtering functions for EM waves at any desired frequency band [1]. These periodic cell structures can be used as low-pass, high-pass, band-pass, and band-stop filtering operations. FSS structure is generally composed of metallic periodic resonators placed on a dielectric layer. For our purpose, a dual-band FSS structure providing band-pass response was designed and analyzed on a 3D-printed substrate layer on a radome. With the increasing need in the communication field, electromagnetic interference has become a significant problem, particularly in hospitals, government buildings, military facilities and so on where high sensitivity is needed. Such demand yielded a growing interest in using artificial materials to obtain more efficient results that cannot be obtained from natural materials.

Through a literature review, it is observed that there are some studies on FSS design using 3-D printing technology with various purposes. In a study, Deepika et al. studied FSS printed with acrylonitrile butadiene styrene plastic material using 3-D printers for radar applications [2]. In another study, Singh et al. developed a

* Corresponding author: mete.bakir@tai.com.tr. ORCID Number of authors: [1,2] 0000-0002-5044-3104

circular loop FSS structure with the help of 3-D printers by using ABS material and circular loop shape structures [3]. In another study, Alvarez et al. investigated a 3-D conformal bandpass FSS operating at 26-40 GHz [4]. In addition, Izquierdo et al. developed a 3D folded dipole FSS structure for electromagnetic structure control [5]. Moreover, there are studies on the use of 3D technology in a lot of electromagnetic applications including radome structures for various antenna types and frequency bands [6-8]. This technology is also studied on different antenna parts such as the ground plane. Such applications are usually called electromagnetic band gap (EBG) structures [9].

In general, the FSS structure is designed and manufactured on planar surfaces using an FR-4 type substrate as the dielectric layer, and copper is generally used for the resonator structure. However, this approach is challenging and expensive if FSS structures will be placed on a curved surface or any non-planar zones. For this purpose, conductive paint and graphite were also examined and the obtained performances are compared by taking copper as the reference. This study focuses on designing an efficient dual-band FSS structure with the help of 3-D printed materials by optimizing conductor type, thickness, and raster orientation of substrate providing band-pass behavior at two frequency bands.

2. Materials and Methods

2.1. Manufacturing 3-D printed samples and Electromagnetic Characterization

For the plastic material of the samples, PLA (Polylactic Acid) filament (MICROZEY PLA, with 1.75 mm diameter) was used. Four samples were printed with different raster orientations as shown in Figure-1 below. The manufactured products have high tensile strength and impact resistance, fast printing ability, and provide very sufficient surface quality. As seen in the figure, the samples have four different configurations of raster orientations. It is well known that raster orientations significantly affect the mechanical strength of the structures.

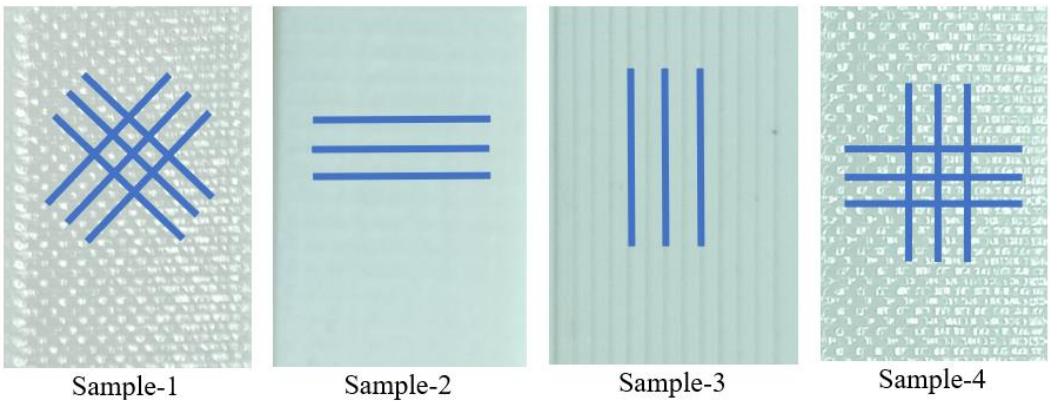

Figure 1. 3-D Printed Samples with different configurations

As seen in the figure, each manufactured sample has different raster orientations while their other properties are kept the same. All samples have 30.0% filler density with 200 °C printing temperature while their raster orientations are 45° Grid for Sample-1, Horizontal Lines for Sample-2, Vertical lines for Sample-3 and 90° Grid for Sample-4.

FSS structures are normally produced on printed circuit boards using FR-4 material as the dielectric substrate. Without exception, all electromagnetic simulation programs have libraries providing electromagnetic properties of well-known and most commonly used dielectric materials. To define the produced samples in the computer environment, their electromagnetic properties have to be determined. Some of the methods for this purpose are free space, dielectric probe method, and waveguide measurement setup. The waveguide measurement system was preferred in this study since it requires samples with smaller dimensions compared to the other methods. The samples shown in Figure-1 have rectangular shapes in the dimensions that can fit waveguide sample holder operating at 12-18 GHz. The waveguide measurement setup contains a 2-port vector network analyzer (VNA), two waveguides with two adaptors and a sample holder to place the samples as shown in Figure 2.

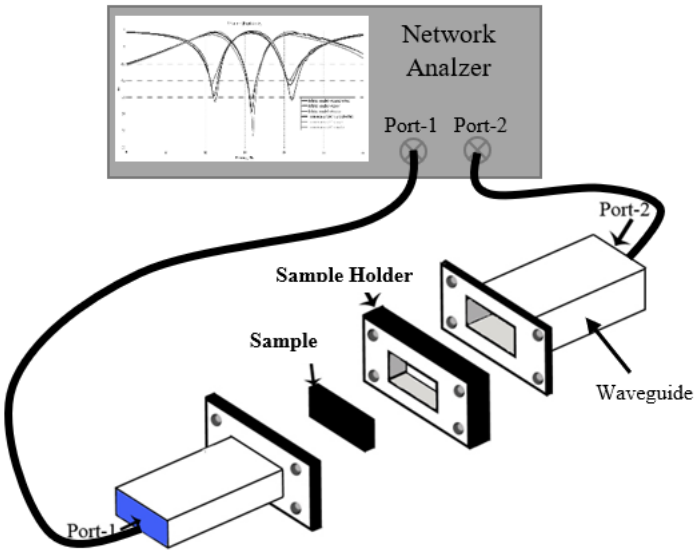

Figure 2. Waveguide test setup used to find electromagnetic characteristics of the samples.

With this test method, scattering parameters (S-parameters) providing reflection and transmission information between ports are obtained. Complex electrical permittivity "ε" and magnetic permeability "μ" values with respect to frequency can be determined by using the obtained S-parameters. One of the most commonly used method is Nicholson Ross Weir (NRW) method which is used in this setup. NRW method was found by scientists; Nicholson, Ross and Weir in their studies [10,11]. In this method, complex "ε" and "μ" values can be found as follows;

$$\mu_r^* = \frac{2\pi}{\Lambda\sqrt{k_0^2 - k_c^2}}\left(\frac{1+\Gamma}{1-\Gamma}\right) \tag{1}$$

$$\varepsilon_r^* = \frac{1}{\mu_r^* k_0^2}\left(\frac{4\pi}{\Lambda^2} + k_c^2\right) \tag{2}$$

Here,

$$\Gamma = X \pm \sqrt{X^2 - 1} \tag{3}$$

$$X = \frac{S_{11}^2 - S_{21}^2 + 1}{2S_{11}} \tag{4}$$

$$T = \frac{S_{11} + S_{21} - \Gamma}{1 - (S_{11} + S_{21})\Gamma} \tag{5}$$

$$\frac{1}{\Lambda^2} = -\left[\frac{1}{2\pi L}\ln(T)\right]^2 \tag{6}$$

After obtaining EM properties of the 3-D printed samples, they were transferred into the electromagnetic simulation program in computer environment. All different combinations with different conductive materials are tested as a substrate for designing the FSS unit cell structure.

2.2. Dual-band FSS Unit Cell Design and Simulation

In this study, we have used diamond shape FSS structure to obtain band-pass behavior. In order to achieve dual-band behavior, the same structure with different sizes were placed in a single cell as shown in Figure-3.

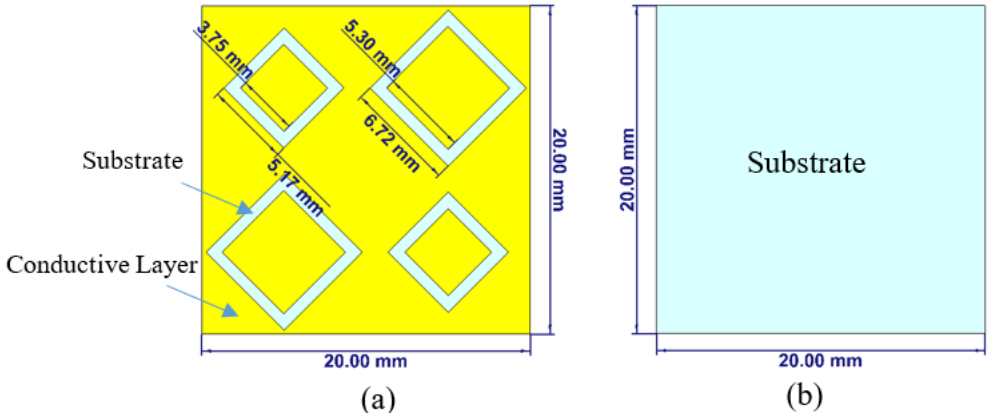

Figure 3. Front (a) and back (b) side of the dual band FSS cell structure.

FSS structures are composed of conductive and dielectric layers. In order to design and manufacture an FSS structure, a conductive material must be used on top of the substrate. Most FSS applications in literature and industry are based on planar surfaces. However, there is a need to integrate these periodic structures on non-planar surfaces such as radomes. Therefore, a conductive material with sufficient reflection behavior is needed since conventional methods will be hard and expensive to apply on curved surfaces. At this point, conductive paint has become a very reliable candidate for replacing copper in this type of structure. In general, metal-based pigments (copper, aluminum, zinc, silver etc.) are found in conductive paint products while there are other and different formulations providing conductivity. These types of paints are widely used in different industries including aerospace and automotive. By reviewing related literature and commercial products, the most suitable conductive paint candidate was determined. During this selection, particularly surface resistance value stated in the technical datasheet of the products was taken into consideration. The conductive paint selected for this study is a copper-based product having two component, 3-part binder, and 1.6 g/cm3 specific gravity value. In terms of surface resistance, the paint has 0.3 Ω/sq value after final curing period. For comparison, graphite was also used for the replacement of copper and the results for all cases are obtained using CST Microwave Studio.

3. Results and Discussion

The results will be discussed for four main cases depending on the material used for the dielectric layer of FSS. In this context, Sample-1 was used as the substrate in the first case while Sample-2, Sample-3, and Sample-4 were used for the second and third cases. Each case includes the use of copper, conductive paint, and graphite as the resonator layer (conductive layer) of FSS. Substrates built by using 3D printed samples were used and compared for all cases in order to achieve maximum efficiency for radome applications. The obtained results for the first case are given in the following figure (Figure 4). As seen in the figure, using 3D-printed samples as the substrate, we have successfully obtained band-pass behavior at two separate frequency bands. The figure provides the reflection and transmission behavior for Sample-1 with different conducting layers including copper, conductive paint, and graphite. It can be clearly seen that copper provides the best solution but conductive paint and graphite also provide very close behavior. For a better understanding, it should be noted that 0 dB for reflection refers to 100% reflection while -10dB corresponds to 10% reflection. On the other hand, 0dB for transmission refers to 100% transmission of the signal sent from one port to the other while -10dB corresponds to that 10% of the signal is transmitted to the other port. In this context, signals are transmitted more than 95% at around f=12.5 GHz and f=16.3 GHz while the reflection behavior also supports this filtering property.

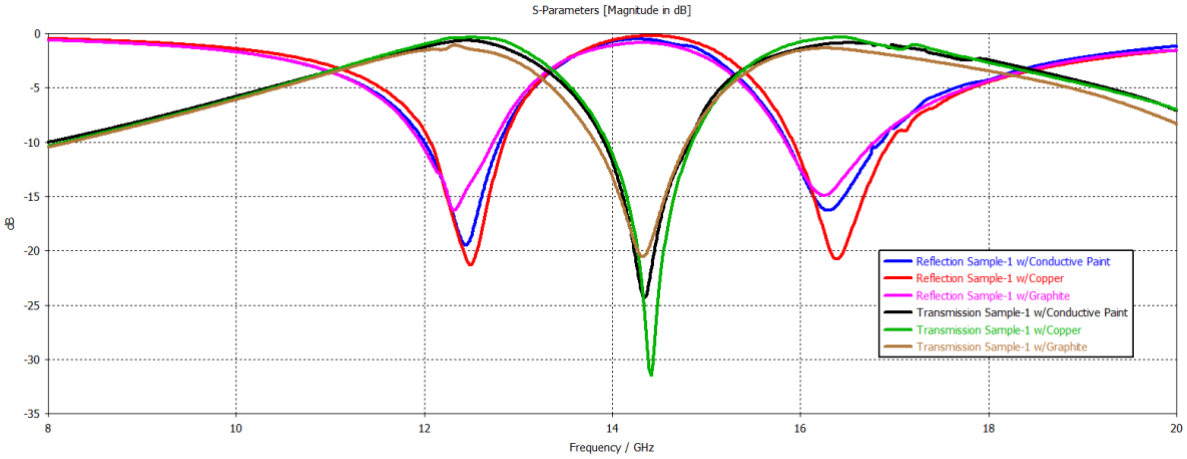

Figure 4. Reflection and Transmission behavior of FSS with Sample-1 as the substrate

For the second case, if we change the substrate from Sample-1 to Sample-2, the following transmission and reflection behavior is obtained (Figure 5). As seen in the figure, using conductive paint slightly shifted the filtering band to lower frequencies but it should be noted that the FSS cell structure can be adjusted to work at any frequency range. Therefore, this shift can be adjusted depending on the need. Overall, behavior is very close to the copper case especially at the 1st band pass part.

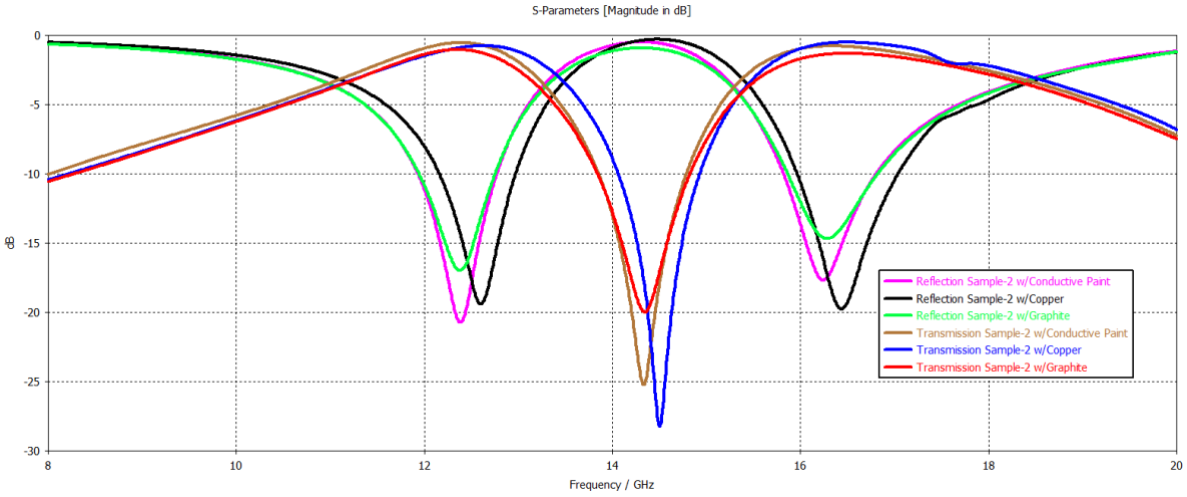

Figure 5. Reflection and Transmission behavior of FSS with Sample-2 as the substrate

For the third case, the substrate layer changed to Sample-3 with vertical lines and the obtained reflection and transmission behaviors are drawn in the figure below (Figure 6). There are some oscillations on the curves due to the vertical raster orientations. Since the signals sent from the ports are also vertically polarized, this distortion can be explained by this co-polar behavior.

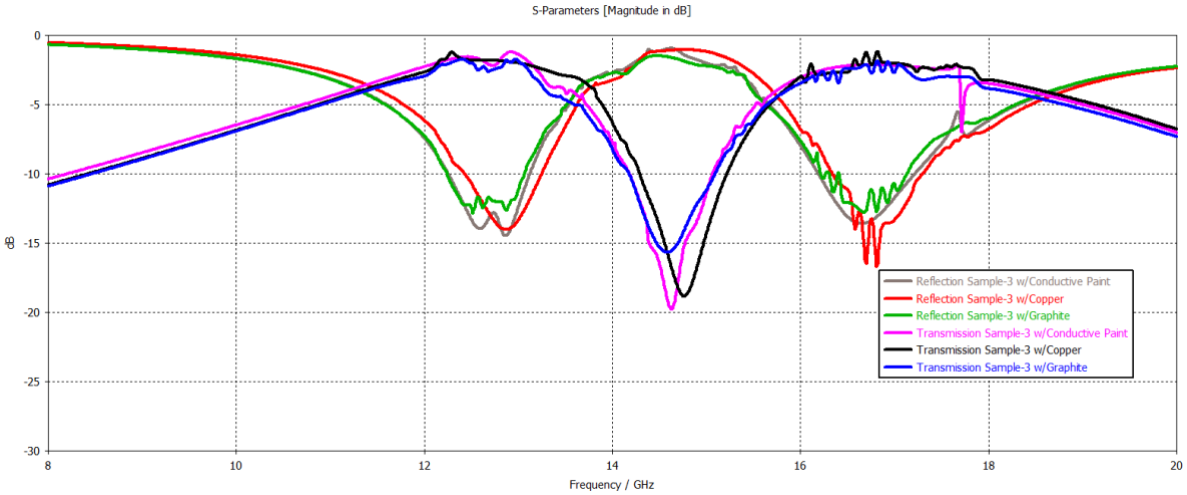

Figure 6. Reflection and Transmission behavior of FSS with Sample-3 as the substrate

For the last case, the dielectric substrate of the proposed dual-band FSS structure was changed to Sample-4 with 90° grid configuration. The obtained transmission and reflection values are plotted in Figure 7 below. Unlike the Sample 1 which also has a grid configuration, Sample-5 yields some small oscillation at the band-pass filtering points. This oscillation is a slightly higher for conductive paint but the overall behavior remains the same. The oscillation can also be explained by the grid angle and the polarization of the incoming wave sent by the ports as in the previous case. The structure will provide band-pass behavior at the corresponding frequencies.

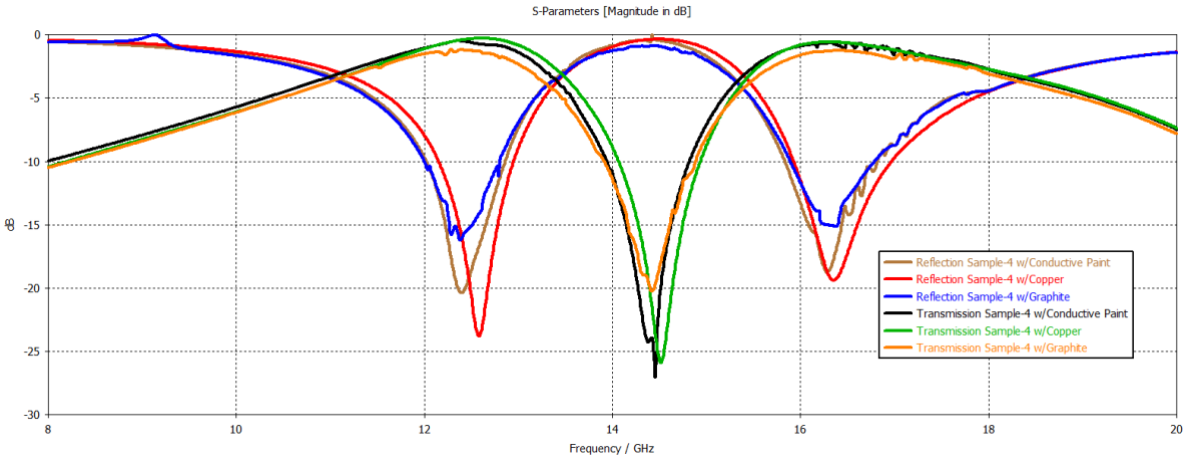

Figure 7. Reflection and Transmission behavior of FSS with Sample-3 as the substrate

For a better understanding the effect of resonator size, e-field distributions for low band (f=12.5 GHz) and high band (f=16.4 GHz) were plotted for the first case (Sample-1) with copper conductive layer (Figure 8). Plotting was only made for one case and for one conductive material only since that would be sufficient to show the corresponding effect. As seen in the figure, larger structures are active for the low band while smaller structures become active at the high band which is an expected results due to the wavelengths.

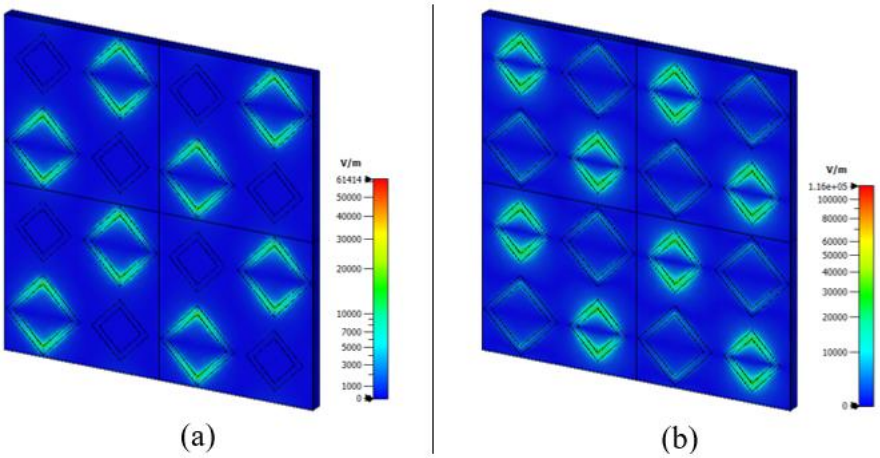

Figure 8. E-field distribution for f=12.5 GHz and f=16.4 GHz

In order to clarify the comparison among the different samples used for the substrate and the materials used for the conductive layer, maximum transmission and minimum reflection responses of all cases for two separate filtering bands are tabulated below (Table-1).

Table 1. Maximum transmission and minimum reflection values of the designed structure

Sample	Configuration	1st Frequency Band						2nd Frequency Band					
		Max. Transmission (dB)			Min. Reflection (dB)			Max. Transmission (dB)			Min. Reflection (dB)		
		Copper	C. Paint	Graphite	Copper	C. Paint	Graphite	Copper	C. Paint	Graphite	Copper	C. Paint	Graphite
#1	45° Grid	-0.37	-0.64	-1.06	-21.23	-19.45	-16.27	-0.34	-0.86	-1.34	-20.72	-16.27	-14.89
#2	Horizontal Lines	-0.74	-0.51	-1.02	-19.33	-20.74	-16.96	-0.49	-0.75	-1.29	-19.75	-17.66	-14.66
#3	Vertical Lines	-1.18	-1.19	-1.70	-14.01	-14.46	-12.85	-1.14	-2.11	-1.84	-16.72	-13.57	-12.75
#4	90° Grid	-0.29	-0.49	-1.15	-23.78	-20.38	-16.23	-0.59	-0.63	-1.26	-19.35	-18.72	-15.13

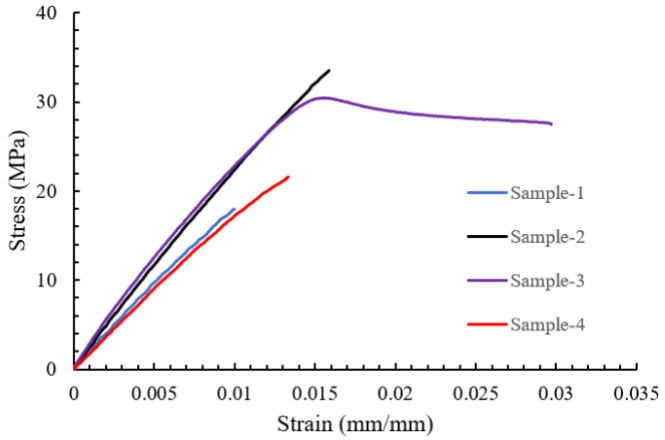

Figure 9 Mechanical test results for tensile loading configuration

Figure 9 shows the tensile test results for four different sample configurations. Sample-1, with a 45° grid layout, demonstrates 18.0 MPa of tensile strength and 1.0 % of strain that yields a 2.0 MPa of Young's Modulus. As well, Sample-2, having a horizontal line configuration, shows 33.5 MPa of tensile strength and 1.5 % of strain with 2.4 MPa of Young's Modulus. It is clear that the single preferential orientation of filaments positively affects the mechanical performance. Sample-3, with a vertical layout, yields 30.4 MPa of tensile strength and 3.0 % of strain, corresponding to 2.7 MPa of Young's Modulus. By comparing Sample-2 and Sample-3, it is worthwhile to underline that selective orientation along the stress direction improves the plastic deformation capacity, observed

as a higher strain. Sample-4, having 90° grid layout, demonstrates 21.6 MPa of tensile strength and 1.3 % of strain that yields a 1.8 MPa of Young's Modulus. Overall, in line with the electromagnetic analysis, different raster orientations for the plastic substrate differ in mechanical properties due in part to stress distribution along filament position and structural variety to bulk material configuration.

4. Conclusion

In conclusion, a dual-band, diamond shape frequency selective surface was designed using 3-D printed substrates. Different raster orientations along with different conductive layers including copper, conductive paint and graphite were examined. The mechanical properties of the samples were also found. Overall, it can be said that Sample-1 and Sample-4 provide the best filtering behavior for all conductive layer types we have used. Although copper provides smoother and better transmission and reflection behavior, conductive paint will provide the ability to manufacture non-planar radomes more easily at lower cost. This combination can be considered as a good candidate, particularly for more complex radome shapes.

References

[1] Munk BA. Frequency selective surfaces: theory and design. New York: Wiley; 2005.
[2] Deepika S, Rana P.Y. A 3-D printed square loop frequency selective surface for harmonic radar applications. J Electromagn Waves Appl 2020; 34(3): 396-406.
[3] Deepika S, Abhinav J, Rana PY. Development of Circular Loop Frequency selective surface using 3-D printing technique. Prog Electromagn Res M Pier M 2020; 90: 195-203.
[4] Alvarez HF, Cadman DA, Goulas A, de Cos Gomez ME, Engstrom DS, Vardaxoglou JC, Zhang S. 3D conformal bandpass millimeter-wave frequency selective surface with improved fields of view. Sci Rep 2021; 11: 12846.
[5] Sanz-Izquierdo B, Parker EA. 3-D Printing of Elements in Frequency Selective Array. IEEE Trans Antennas Propag 2014; 62(12): 6060.
[6] Sudhendra C, Madhu AR, Mahesh A, Pillai ACR. FSS Radomes for Antenna RCS Reduction. Int J Adv Eng Technol 2013; 6(4):1464-1473.
[7] Omar AA, Shen Z. Thin 3-D bandpass frequency-selective structure based on folded substrate for conformal radome applications. IEEE Trans Antennas Propag 2019: 67(1); 282-290.
[8] Park CS et al. Analysis of curved frequency selective surface for radome using characteristic basis function method. EuCAP 2016: 2-5.
[9] Jun S, Sanz-Izquierdo B. A CPW-fed Antenna on 3D Printed EBG Substrate. LAPC 2015:1-5.
[10] Nicolson AM, Ross GF. Measurement of the intrinsic properties of materials by time-domain techniques. IEEE Trans Instrum Meas 1970; 19: 377–382.
[11] Weir WB. Automatic measurement of complex dielectric constant and permeability at microwave frequencies. Proc IEEE 1974; 62: 33–36.